Science Advances

Supplementary Materials for

A stable Atlantic Meridional Overturning Circulation in a changing North Atlantic Ocean since the 1990s

Yao Fu, Feili Li*, Johannes Karstensen, Chunzai Wang*

*Corresponding author. Email: cwang@scsio.ac.cn (C.W.); feili.li@gatech.edu (F.L.)

This PDF file includes:

Data description
Figs. S1 to S12
Tables S1 to S6

Data Description

A05 section along 24.5°N

The World Ocean Circulation Experiments (WOCE) A05 line nominally along 24.5°N, aligning closely with the latitude of the RAPID array, has been repeated several times since the 1990s. In this study, we use the repeats in 1992, 1998, 2004, 2010, 2011, and 2015 (Table S1). The Conductivity-Temperature-Depth (CTD) data of the repeats are provided by the CLIVAR and Carbon Hydrographic Data Office (CCHDO, at https://cchdo.ucsd.edu/). All the CTD profiles, including temperature, salinity, and dissolved oxygen data, reached tens of meters above the sea floor. The original data have 2-m vertical resolution and are linearly interpolated into 1-m resolution prior to the calculations. The averaged distance between adjacent CTD profiles for the different repeats is 20 to 25 nautical miles. When the cruise was sampling the boundary currents and crossing the continental shelf, the distance is reduced to about 10 nautical miles to obtain a finer resolution.

Eastern subpolar North Atlantic section

The eastern subpolar North Atlantic (SPNA) section consists primarily of the WOCE AR7E line and the recently occupied OSNAP-East line (available through CCHDO at https://cchdo.ucsd.edu/ and British Oceanographic Data Centre at https://www.bodc.ac.uk/). The AR7E line runs from the southern tip of Greenland to Ireland or Scotland with multiple repeats since the early 1990s (Fig. 1 and Table S2). The section is designed to continuously monitor hydrographic and overturning changes in the eastern SPNA, and has been recently succeeded by the OSNAP project. The cruise tracks of the AR7E section differ slightly from year to year. In the Irminger Basin (from Greenland to the Reykjanes Ridge), all the repeats followed nearly an identical track. To the east of the Reykjanes Ridge, the repeats in 1992, 1995, 1996 and 1997, carried out under the German WOCE program, followed a detour toward the southeast direction in the Iceland basin and then turned eastward to the shelf of Ireland; the rest of the repeats continued in the east-southeast direction to North Ireland or to Scotland. Temperature and salinity were

measured during all the repeats, while oxygen was available in the repeats of 1991, 1992, 1997, 2007, 2011, and 2014. Despite the slight differences in cruise tracks, the water mass composition in the water column of the occupied tracks are nearly identical.

Labrador Section

The Labrador section used in this study is composed of the WOCE line of AR7W and the OSNAP-West line (available through CCHDO at https://cchdo.ucsd.edu/ and Pangaea at http://www.pangaea.de/expeditions/cr.php/Merian). The AR7W line, running from the Labrador shelf to the western shelf of Greenland (Figure 1), is occupied almost annually in the late spring and early summer. The operation along this line extended beyond the WOCE program and is still ongoing. The OSNAP-West line follows the OSNAP-West array position and deviates from the AR7W line in position. The AR7W line cuts through the central Labrador Sea focusing on the convection and water mass property changes in the Labrador Sea, while the OSNAP-West line runs along the outer skirt of the Labrador Sea focusing on the overturning transport in the Labrador Sea. As a result, one may expect a slightly different overturning structure between the AR7W and OSNAP-West lines. For all the repeats, temperature and salinity were measured using CTD profiles reaching tens of meters above ocean bottom. Dissolved oxygen data were available for most of the repeats (Table S3).

GECCO2 ocean state estimate

The GECCO2 ocean state estimate is the second version of the German contribution to the Massachusetts Institute of Technology general circulation model "Estimating the Circulation and Climate of the Ocean system". GECCO2 has 50 vertical levels, a zonal resolution of 1°, and a meridional resolution of $\frac{1}{3}$° in the tropics and approximately isotropic cells between 20° and 60°. GECCO2 also includes the Arctic Ocean with $\frac{1}{3}$ ° meridional resolution and a dynamic/thermodynamic sea ice model. The adjoint method is used to assimilate hydrographic and satellite data. Monthly outputs from January 1948 to December 2014 are available through the

Integrate Climate Data Center of University Hamburg at https://icdc.cen.uni-hamburg.de/1/daten/reanalysis-ocean/gecco2.html.

AVISO surface geostrophic velocity and absolute dynamic height

The delayed mode level-4 daily AVISO surface geostrophic velocity and absolute dynamic height data are provided by the AVISO Altimetry Data and available through the Copernicus Marine Environment Monitoring Service at http://marine.copernicus.eu/. In this study, we use the AVISO surface geostrophic velocity to calculate the initial reference velocity for the box inverse model (see Materials and Methods for details). We also use the mean absolute dynamic height (averaged between 1993 and 2018) to produce the background for Figure 1 in the main text.
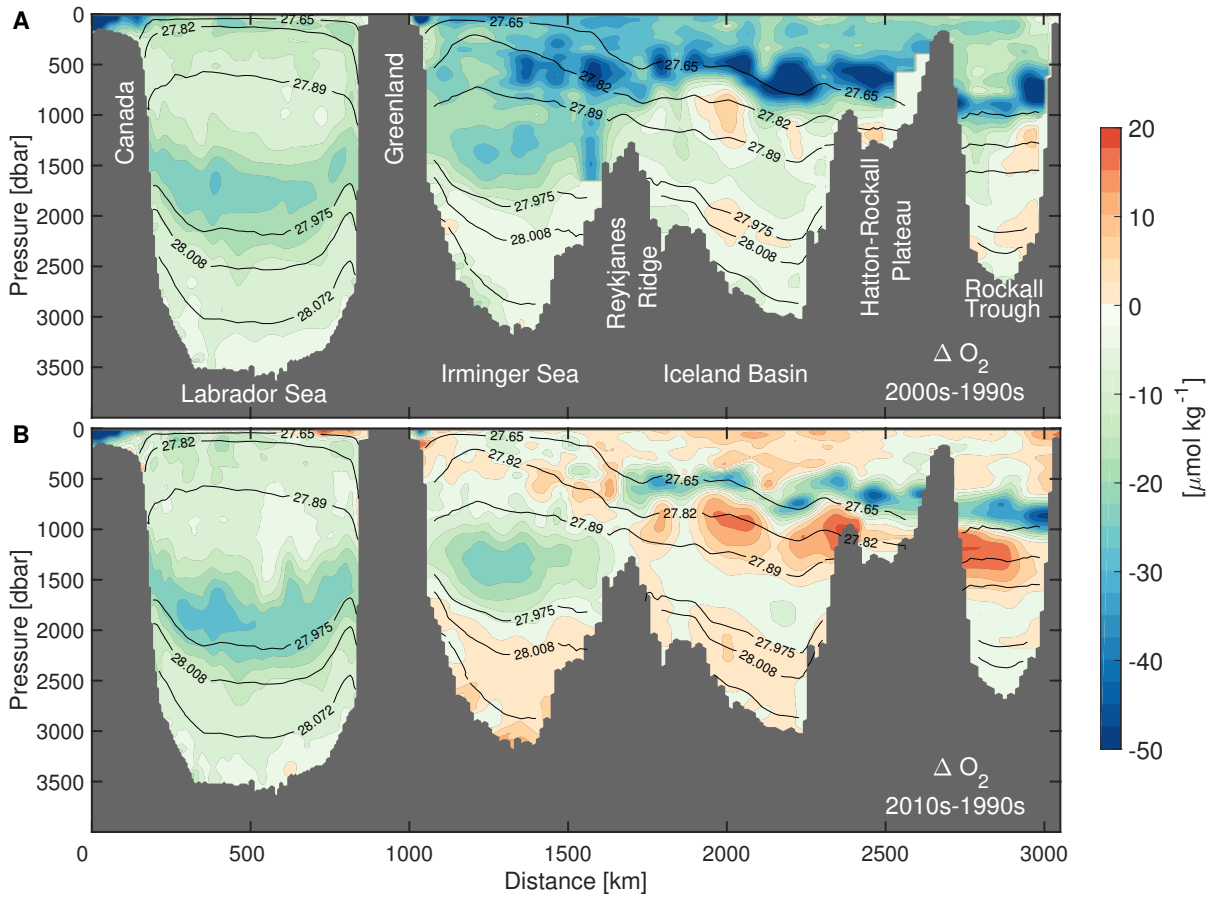
Fig. S1. Decadal dissolved oxygen changes in the SPNA. Dissolved oxygen difference in the subpolar North Atlantic (**A**) between the 2000s and 1990s, and (**B**) between the 2010s and 1990s. The superimposed contours are the mean neutral density surfaces calculated using all the available repeats.

Fig. S2. Decadal potential temperature changes in the SPNA. Potential temperature difference in the subpolar North Atlantic (**A**) between the 2000s and 1990s, and (**B**) between the 2010s and 1990s. The superimposed contours are the mean neutral density surfaces calculated using all the available repeats.
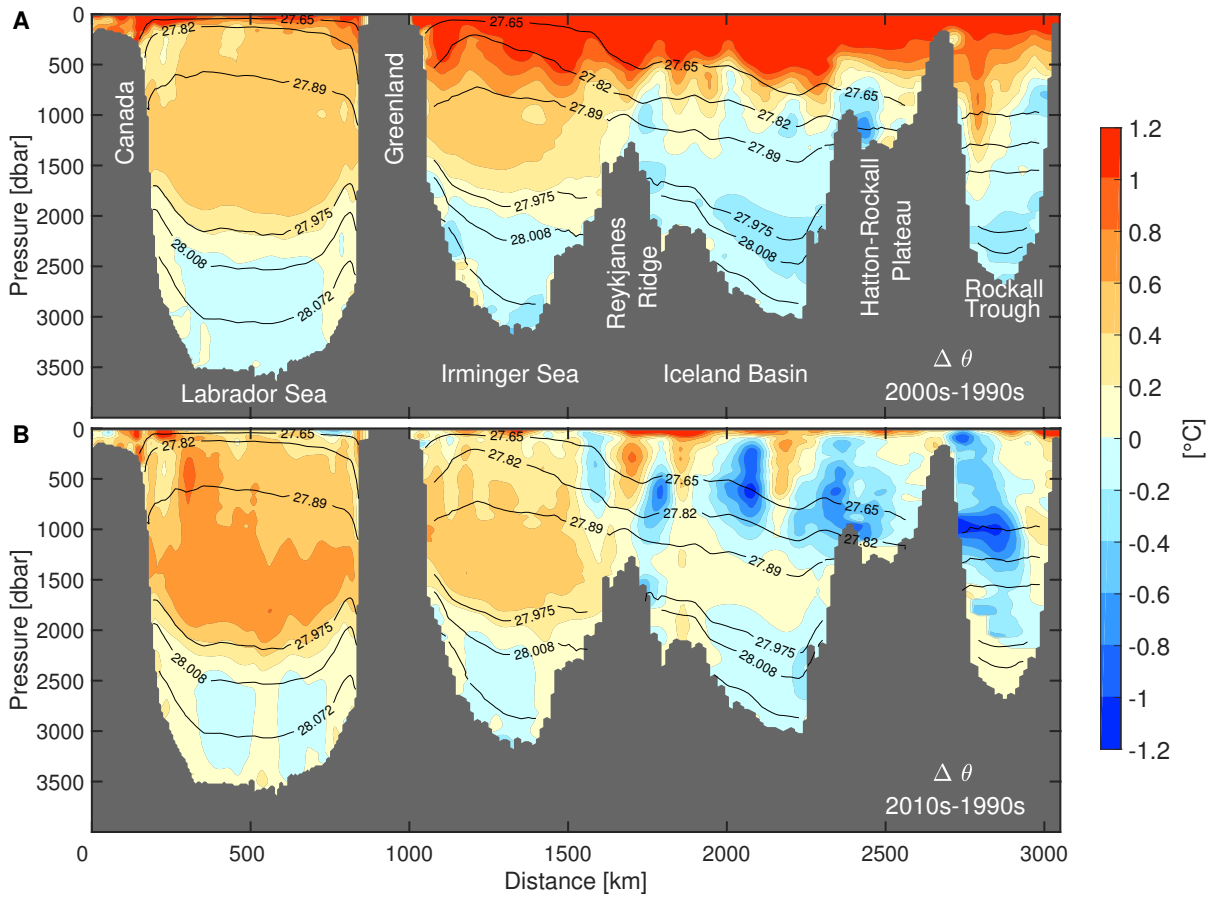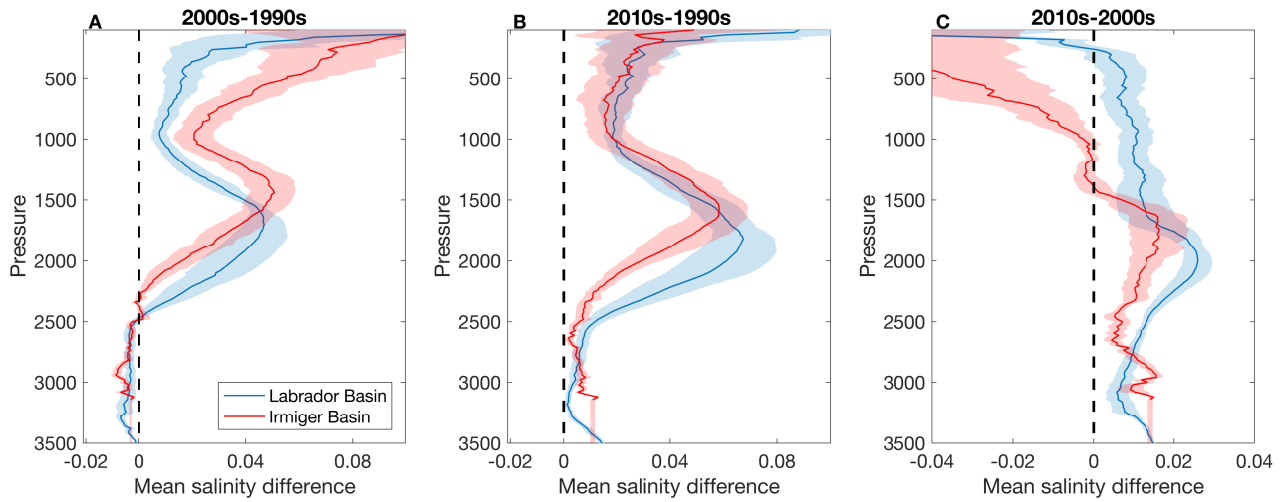
Fig. S3. Section-averaged salinity difference. Section-averaged salinity difference in the Labrador (blue) and Irminger (red) basins between the 2000s and 1990s (**A**), 2010s and 1990s (**B**), and 2010s and 2000s (**C**). Note the scale of *x*-axis in (**C**) is different from that in (**A**) and (**B**). The solid lines represent the section-mean differences in the individual basins, and the shading represents the standard error of the section mean values. The standard error is calculated as the standard deviation of the mean difference divided by $\sqrt{L/\tau}$, where L is the total length of the basin and τ is the integral length scale. τ is calculated by integrating the area between the first positive and negative zero-crossings of the autocorrelation function of individual salinity differences at each depth along the direction of the section.
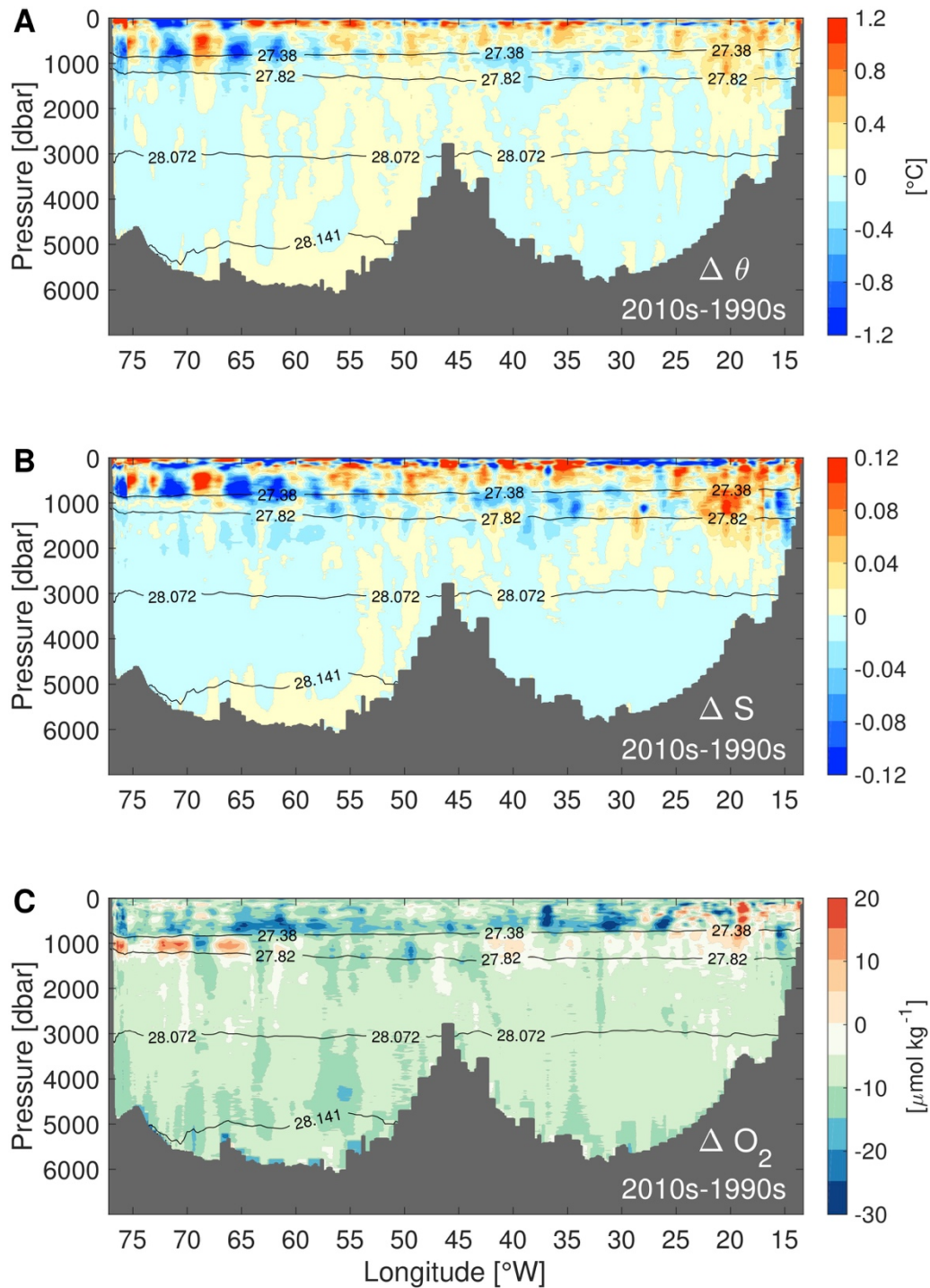
Fig. S4. Decadal hydrographic and oxygen changes in the subtropics. Difference of (**A**) potential temperature, (**B**) salinity, and (**C**) dissolved oxygen at 24.5°N between the 2010s and 1990s. In the subtropics, the most prominent changes in water mass properties between the 2010s and 1990s occur in the deep ocean. Almost the entire NADW water shows freshening, while the Antarctic Bottom Water (AABW) becomes warmer and saltier.
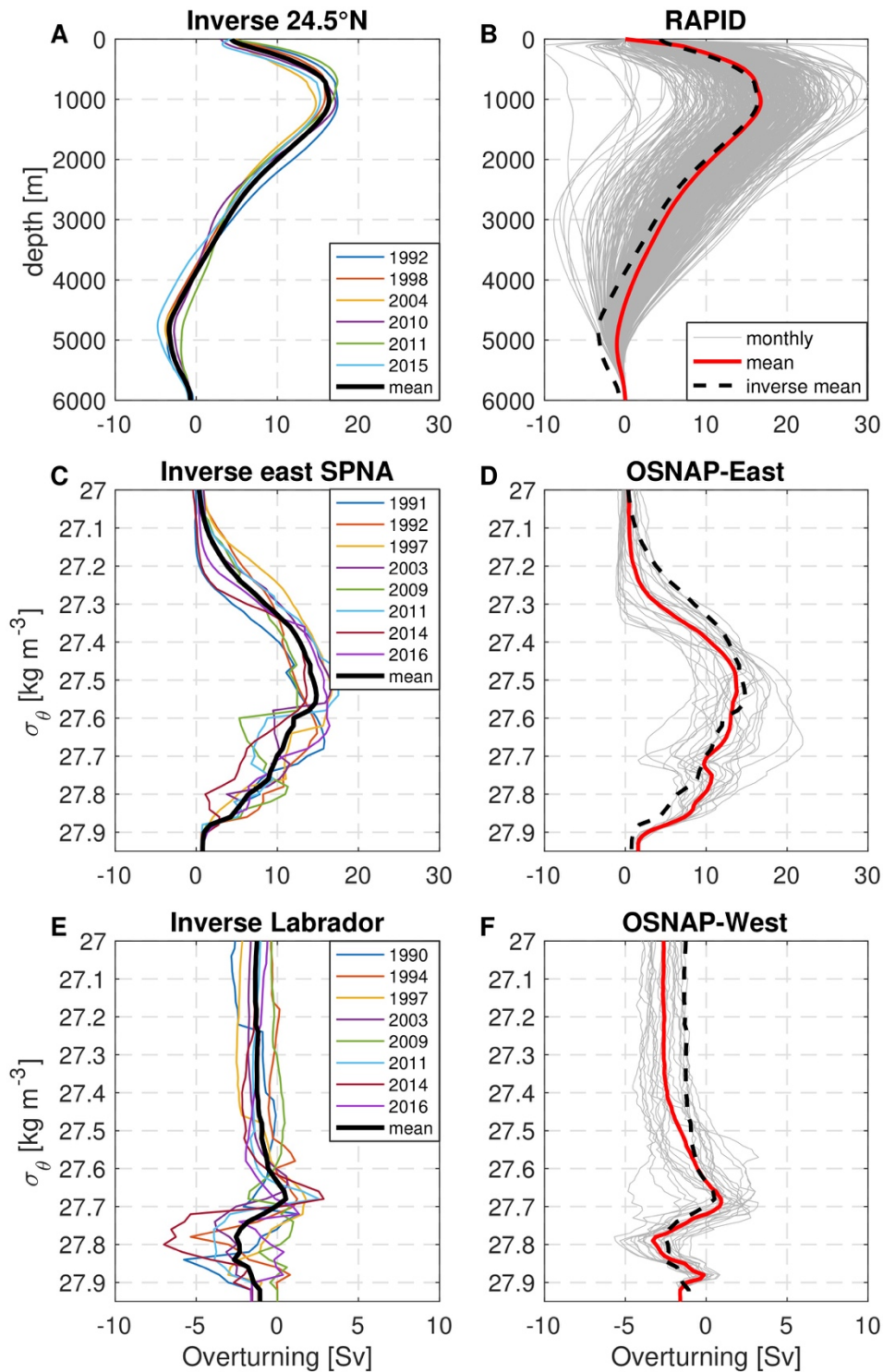
Fig. S5. Overturning streamfunction at each section. Overturning streamfunction of hydrography-based estimates at 24.5°N (**A**), the eastern SPNA section (**C**), and the Labrador section (**E**); and of array-base estimates by RAPID (**B**), OSNAP-East (**D**), and OSNAP-West (**F**). Note that in order to be consistent with the RAPID and OSNAP results, the overturning streamfunction in the subtropical and subpolar North Atlantic is calculated in depth space and potential density space, respectively. The colored lines in (**A**), (**C**), and (**E**) represent the results in the corresponding cruise years, the black thick line represents the mean value of all the repeats. The light gray lines in (**B**), (**D**), and (**F**) are the month results, the red thick lines are the mean in the respective sections, and the black dashed lines are the mean of the hydrography-based estimates and are the same as the black thick line in (**A**), (**C**), and (**E**), respectively.
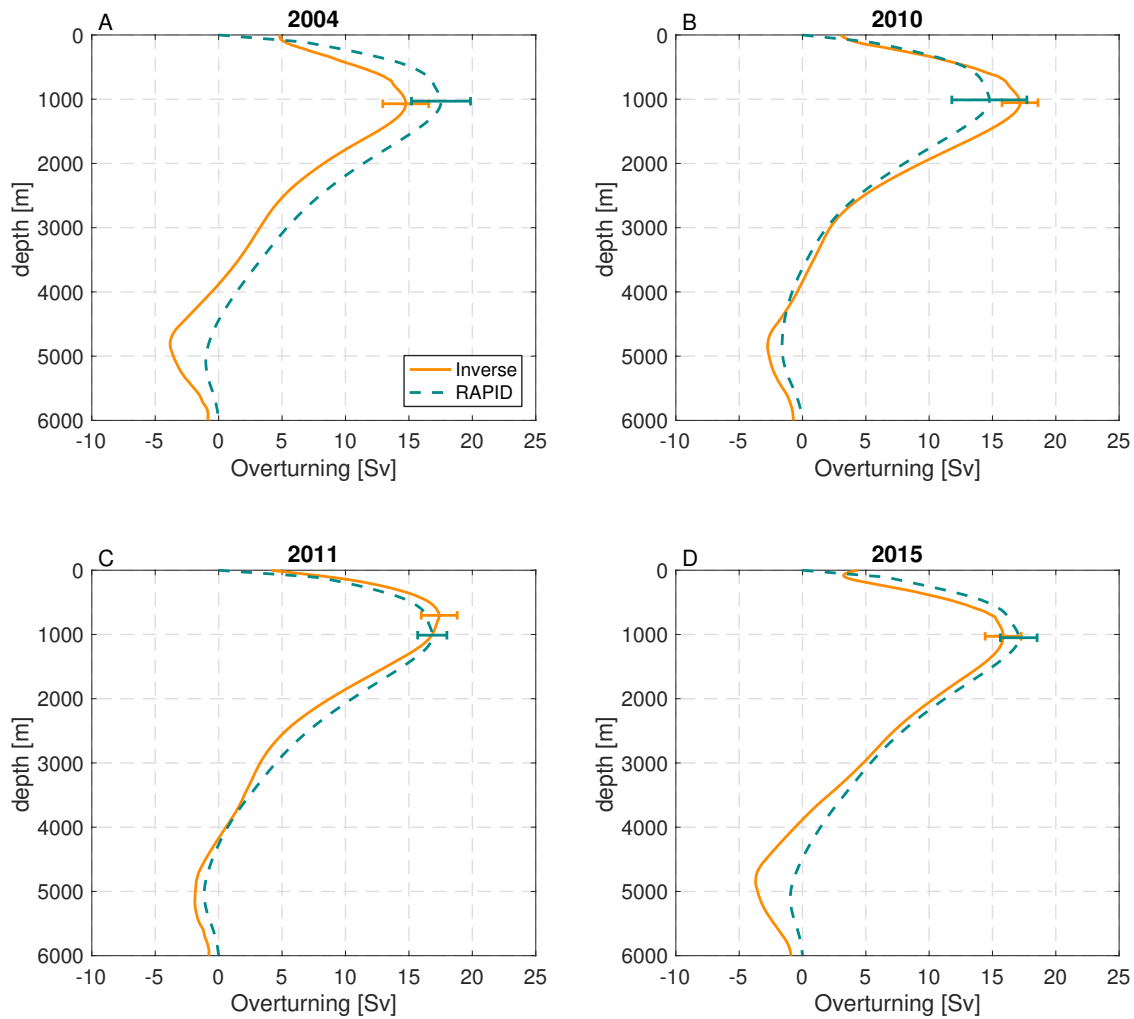
Fig. S6. Overturning streamfunction for RAPID and hydrography at 24.5°N. Annual mean RAPID overturning streamfunction compared with the hydrography-based results in 2004 (**A**), 2010 (**B**), 2011 (**C**), and 2015 (**D**). Error bars are marked at the depth of the maximum overturning streamfunction. The error bars for the RAPID-based results indicate the standard error of the annual mean maximum overturning streamfunction from the monthly values. The error bars for the hydrography-based results are the error covariance matrix of the inverse method.
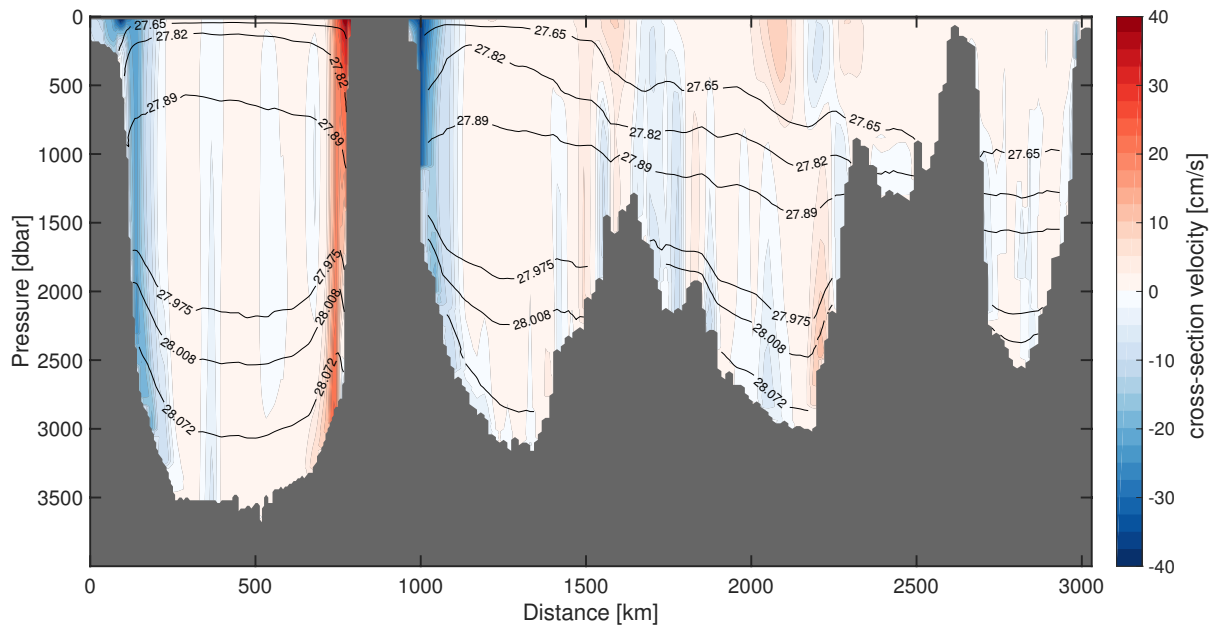
Fig. S7. Mean geostrophic velocity section in the SPNA. Mean absolute cross-section (normal to the section) geostrophic velocity in the SPNA calculated from the hydrography-based estimates. Superimposed contours are the averaged neutral density surfaces. The horizontal coordinate is the distance from Canadian coast. Note that the cruise track differs among the repeats, here we only used the repeats followed similar tracks to produce the mean. For the Labrador section, the 2014 and 2016 repeats are excluded, and for the eastern SPNA section, the 1992 and 1997 repeats are excluded.
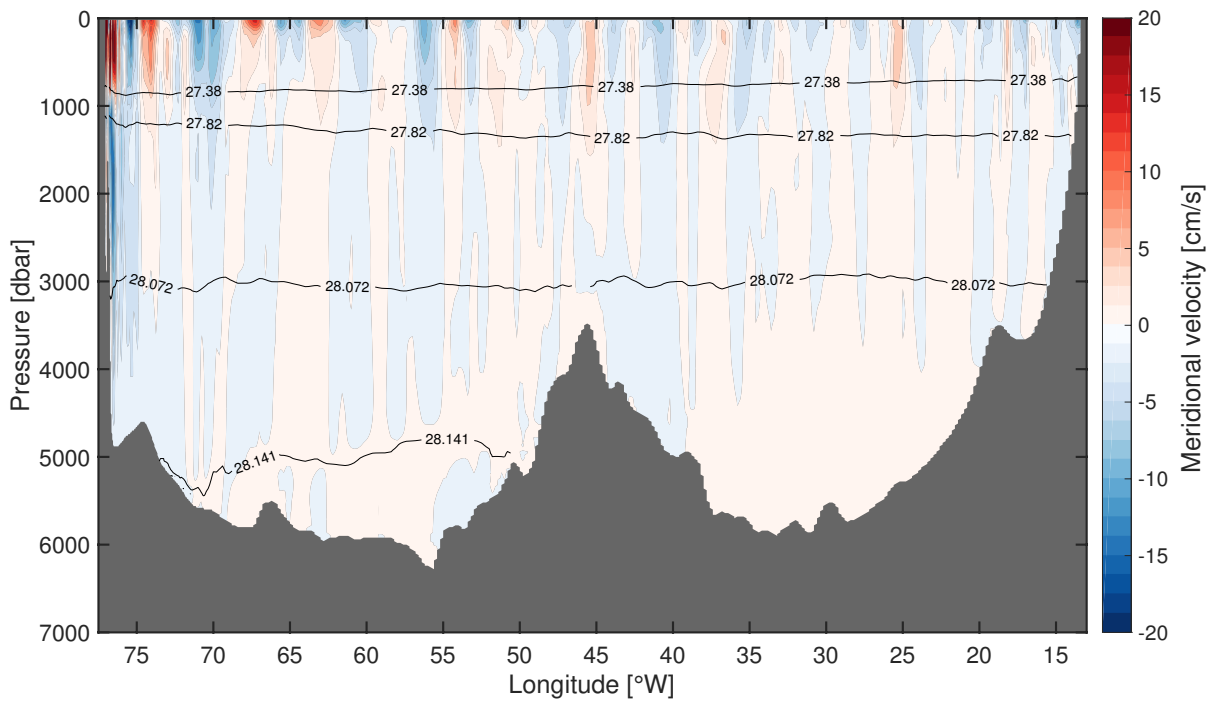
Fig. S8. Mean geostrophic velocity section in the subtropics. Mean absolute meridional geostrophic velocity at 24.5°N calculated from the hydrography-based estimates. Superimposed contours are the averaged neutral density surfaces.
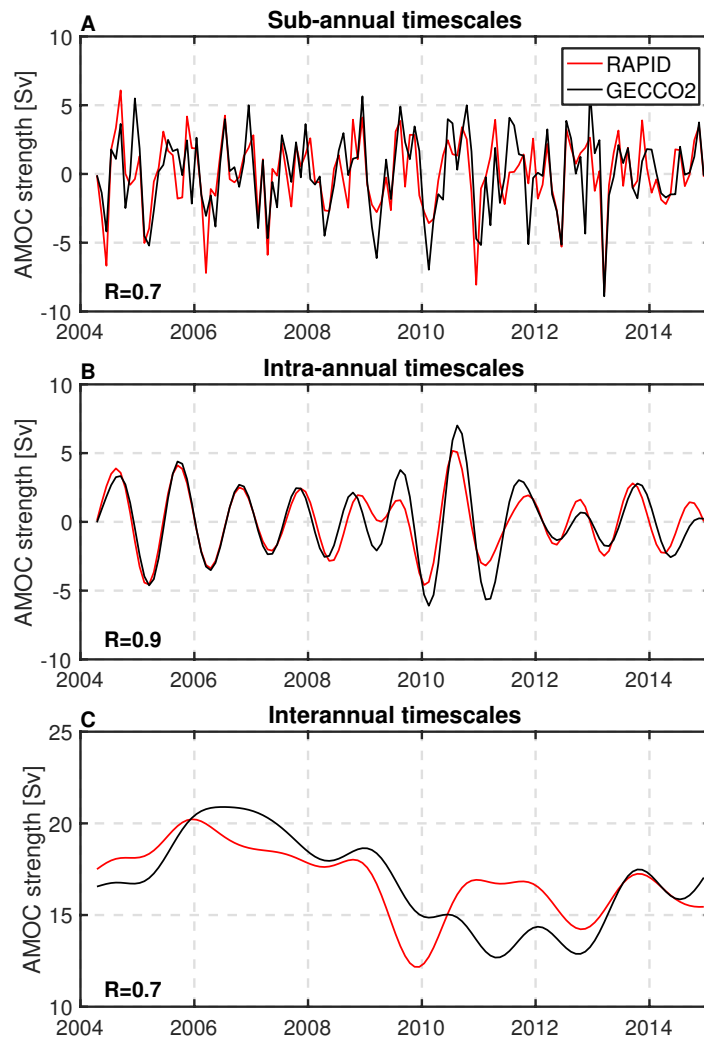
Fig. S9. Comparison of the AMOC variability between GECCO2 and RAPID. The comparison is shown on sub-annual timescales (**A**), intra-annual timescales (**B**), and interannual timescales (**C**). GECCO2 timeseries at 26.5°N is marked by black lines, RAPID by red lines. A 5th order Butterworth filter is applied to the monthly data to obtain the sub-annual timeseries (with periods shorter than 12 months), intra-annual timeseries (with periods between 9 and 24 months), and interannual timeseries (with periods longer than 18 months). The correlation coefficient (significant on 95% significance level) between the GECCO and RAPID timeseries is marked at the lower left corner of each subplot.

Fig. S10. Total subpolar AMOC strength. Total AMOC strength in the SPNA by combining both the Labrador Section and the eastern 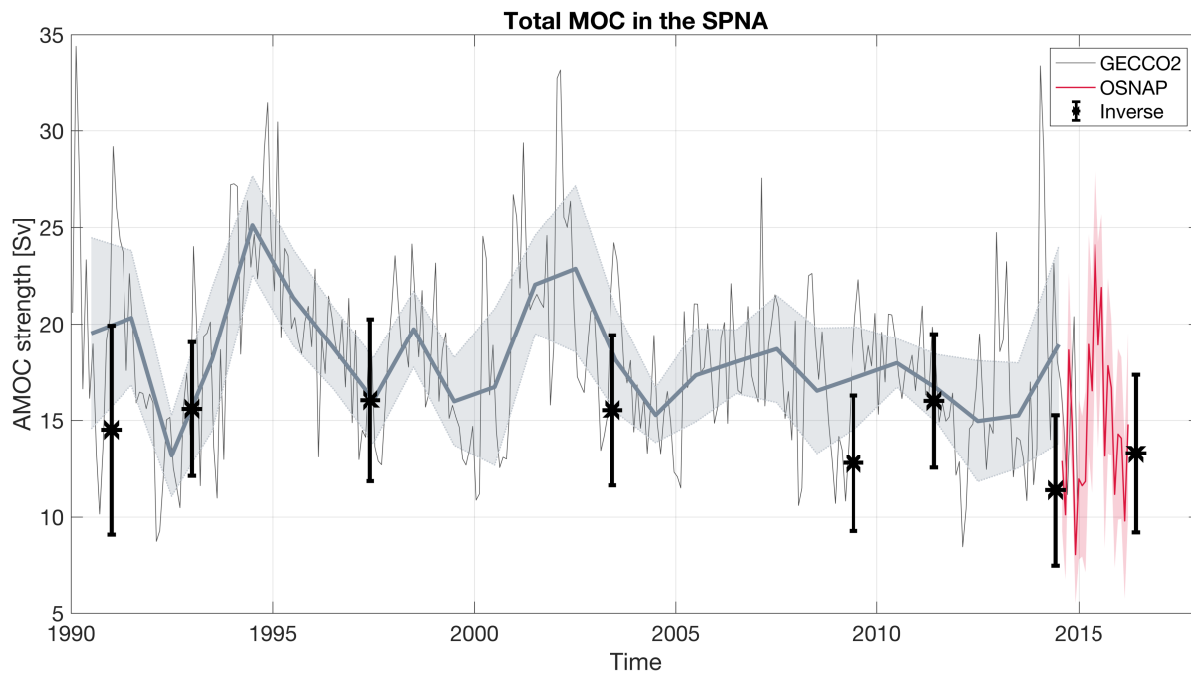SPNA section. The thin gray line is the monthly GECCO2 AMOC strength, and the thick gray line with shades is the annual mean GECCO2 AMOC strength with standard error of the annual mean. The red line is the OSNAP, the asterisks with error bar are the hydrographic based estimates.
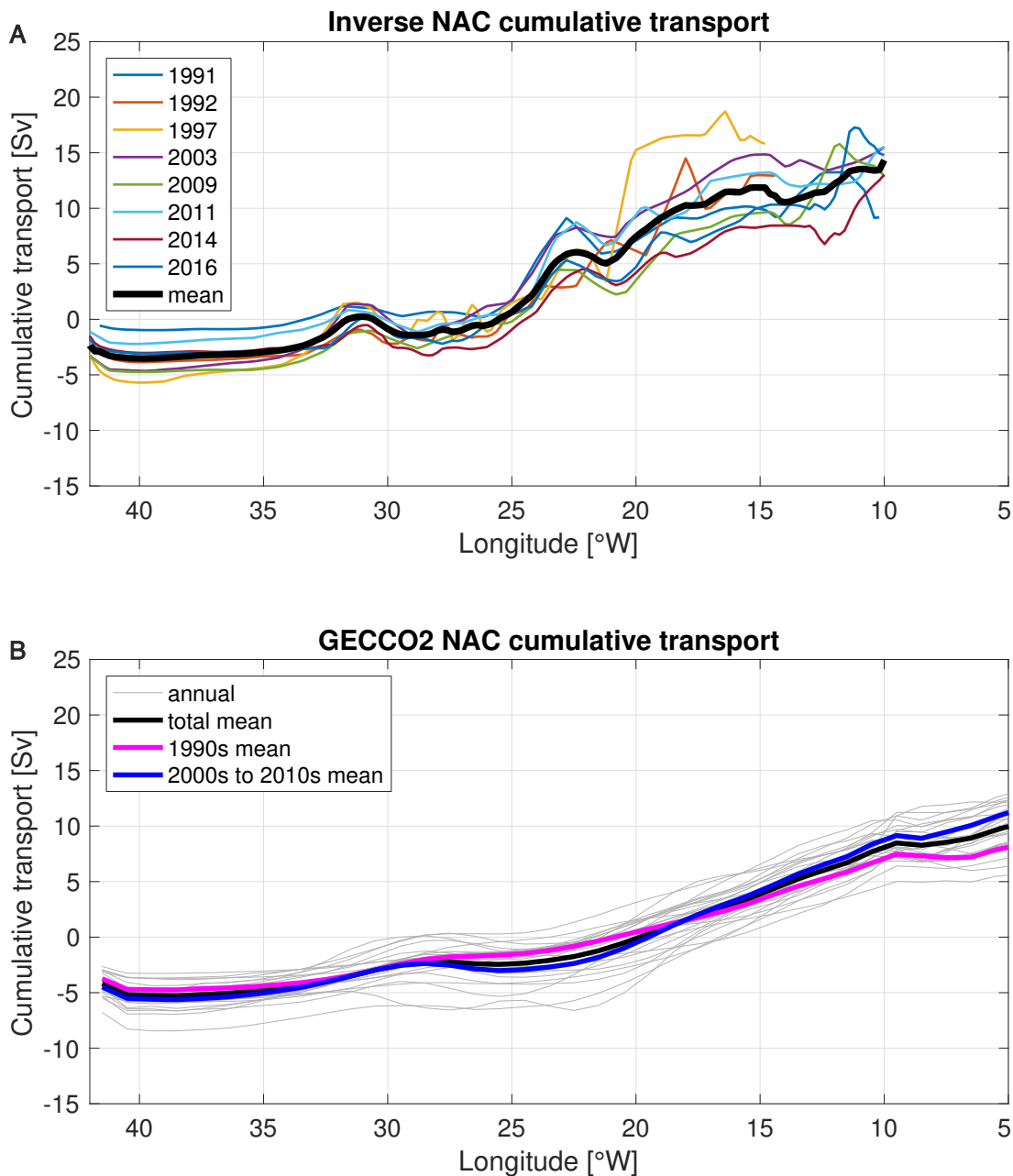
Fig. S11. Cumulative North Atlantic Current transport. Cumulative North Atlantic Current (NAC) transport [Sv] integrated from the west to the east for (**A**) hydrography-based calculation along the cruise tracks of the eastern SPNA section and (**B**) GECCO2 at 59.5°N. The NAC is defined as the transport above the 27.65 km m^{-3} isoneutral (surface of constant neutral density) or equivalently the 27.55 kg m^{-3} isopycnal. In (**A**), the colored thin curves are the estimates of the individual repeats, the black thick curve is the mean of all repeats. In (**B**), the thin gray lines are the annual mean estimates from 1990 to 2014, the black thick line is the mean in this period, the magenta and blue lines are the mean of the 1990s and the 2000s to 2010s, respectively.
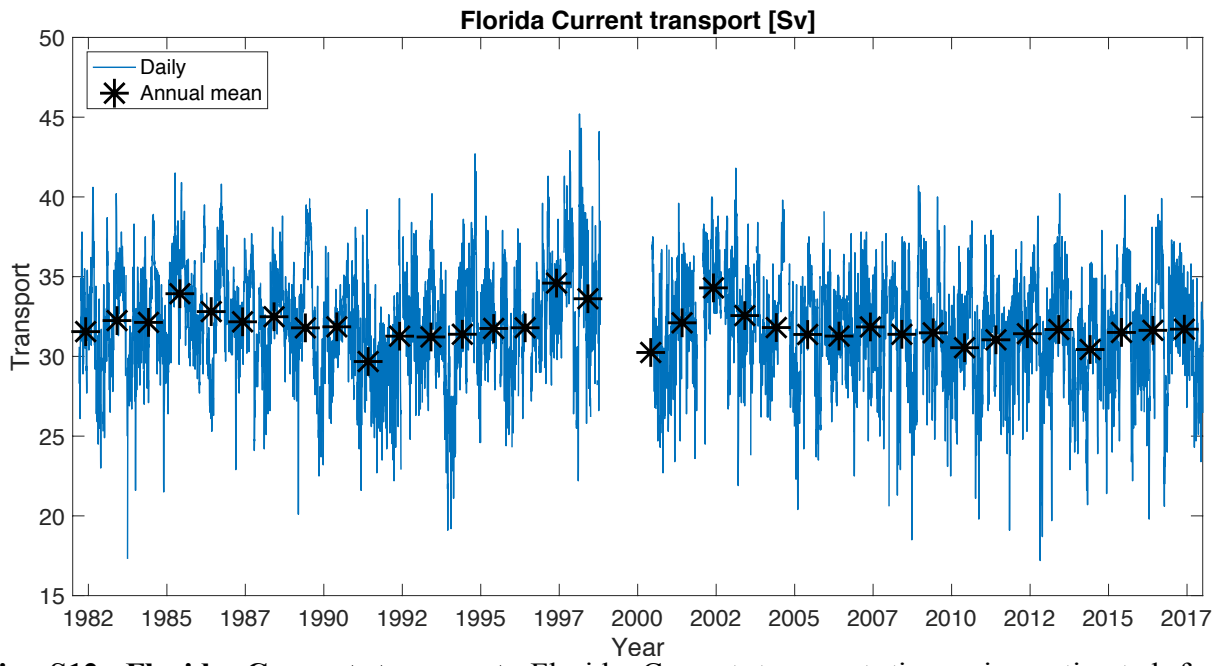
Fig. S12. Florida Current transport. Florida Current transport timeseries estimated from submarine cable voltage data. The dark blue curve is the daily data, the black asterisks represent annual mean value of each calendar year.

Table S1. Cruise list for the subtropical section. Cruise information for the 24.5°N section used in this study. All the repeats contain salinity, temperature, and dissolved oxygen data.

		Subtropical Section		
cruise	date	Principal scientist	Ship and country	Number of stations used
A05-1992	14 Jun 1992 to 15 Aug 1992	G. Parrilla	Hesperides Spain	112
A05-1998	23 Jan 1998 to 24 Feb 1998	D. S. Bitterman and K. Lee	Ronald H. Brown USA	130
A05-2004	04 Apr 2004 to 10 May 2004	S. Cunningham	Discovery UK	122
A05-2010	06 Jan 2010 to 18 Feb 2010	B. King	Discovery UK	132
A05-2011	28 Jan 2011 to 14 Mar 2011	A. Hernandez-Guerra	Sarmiento de Gamboa Spain	166
A05-2015	06 Dec 2015 to 22 Jan 2016	B. King	Discovery UK	132

Table S2. Cruise list for the eastern SPNA section. Cruise information for the eastern SPNA section used in this study. All the repeats contain salinity, temperature data. The repeats marked with "*" contains dissolved oxygen measurement.

		Eastern SPNA Section		
Cruise	Date	Principal scientist	Ship and country	Number of stations used
AR7E-1991-1*	08 Apr 1991 to 01 May 1991	H. M. van Aken	Tyro Netherlands	38
AR7E-1991-2*	01 Aug 1991 to 04 Sep 1991	W. J. Gould	Charles Darwin UK	40
AR7E-1992*	12 Sep 1992 to 06 Oct 1992	A. Sy	Valdivia Germany	54
AR7E-1995	26 May 1995 to 23 Jun 1995	M. Bersch	Valdivia Germany	55
AR7E-1996	19 Aug 1996 to 05 Sep 1996	M. Bersch	Valdivia Germany	54
AR7E-1997*	14 Aug 1997 to 14 Sep 1997	A. Sy	Meteor Germany	35
AR7E-2003	22 Aug 2003 to 10 Sep 2003	H. M. van Aken	PELAGIA Netherlands	41
AR7E-2005	07 Sep 2005 to 05 Oct 2005	C. Veth	PELAGIA Netherlands	29
AR7E-2007*	30 Aug 2007 to 27 Sep 2007	G.-J. Brummer	PELAGIA Netherlands	45
AR7E-2009	24 Sep 2009 to 13 Oct 2009	H. M. van Aken	PELAGIA Netherlands	42
AR7E-2011*	24 Jul 2011 to 08 Aug 2011	H. M. van Aken	PELAGIA Netherlands	43
OSE-2014*	24 Jun 2014 to 21 Jul 2014	B. A. King, N. P. Holliday	James Clark Ross UK	100
OSE-2016	07 Jun 2016 to 17 Aug 2016	N. P. Holliday, S. Cunningham, S. Gary	Discovery UK	120

Table S3. Cruise list for the Labrador section. Cruise information for the Labrador section used in this study. All the repeats contain salinity, temperature. The repeats marked with "*" contains

		Labrador Section		
cruise	date	Principal scientist	Ship and country	Number of stations used
AR7W-1990	02 Jul 1990 to 09 Jul 1990	J. Lazier	Dawson Canada	22
AR7W-1993	17 Jun 1993 to 28 Jun 1993	J. Lazier	Hudson Canada	21
AR7W-1994*	24 May 1994 to 12 Jun 1994	J. Lazier	Hudson Canada	29
AR7W-1996*	12 May 1996 to 01 Jun 1996	J. Lazier	Hudson Canada	29
AR7W-1997*	09 May 1997 to 11 Jun 1997	R. A. Clarke	Hudson Canada	23
AR7W-1998*	22 Jun 1998 to 09 Jun 1998	E. P. Jones	Hudson Canada	16
AR7W-1999*	27 Jun 1999 to 12 Jul 1999	R. A. Clarke	Hudson Canada	24
AR7W-2001*	30 May 2001 to 15 Jun 2001	R. A. Clarke	Hudson Canada	23
AR7W-2002*	23 Jun 2002 to 19 Jul 2002	R. A. Clarke	Hudson Canada	31
AR7W-2003*	13 Jul 2003 to 04 Aug 2003	R. A. Clarke	Hudson Canada	24
AR7W-2004*	15 May 2004 to 30 May 2004	G. Harrison	Hudson Canada	29
AR7W-2005*	26 May 2005 to 07 Jun 2005	G. Harrison	Hudson Canada	31
AR7W-2006*	24 May 2006 to 08 Jun 2006	R. M. Hendry	Hudson Canada	30
AR7W-2008*	20 May 2008 to 04 Jun 2008	G. Harrison	Hudson Canada	22
AR7W-2009*	17 May 2009 to 01 Jun 2009	R. M. Hendry	Hudson Canada	23
AR7W-2010*	13 May 2010 to 30 May 2010	G. Harrison	Hudson Canada	25
AR7W-2011*	06 May 2011 to 29 May 2011	I. Yashayaev	Hudson Canada	28
AR7W-2012*	01 Jun 2012 to 17 Jun 2012	I. Yashayaev	Martha L. Black Canada	36
AR7W-2013*	05 May 2013 to 28 May 2013	I. Yashayaev	Hudson Canada	33
OSW-2014*	09 Jun 2014 to 21 Jun 2014	B. A. King N. P. Holliday	James Clark Ross UK	30
AR7W-2015*	04 May 2015 to 24 May 2015	I. Yashayaev	Hudson Canada	34
OSW-2016*	14 May 2016 to 27 May 2016	J. Karstensen	Maria S. Merian Germany	35

dissolved oxygen measurement.

Table S4. Combination of sections for the inverse calculation. Repeats of each section used for the box inverse calculation. Note that each of the A05-1992 and A05-2015 repeats is used twice to increase the number of estimates in the subpolar North Atlantic.

Inverse box number	Subtropical section	Eastern SPNA section	Labrador section
1	A05-1992	AR7E-1991-2	AR7W-1990
2	A05-1992	AR7E-1992	AR7W-1994
3	A05-1998	AR7E-1997	AR7W-1997
4	A05-2004	AR7E-2003	AR7W-2003
5	A05-2010	AR7E-2009	AR7W-2009
6	A05-2011	AR7E-2011	AR7W-2011
7	A05-2015	OSE-2014	OSW-2014
8	A05-2015	OSE-2016	OSW-2016

Table S5. Neutral density layer interfaces. Neutral density surfaces (γ_n in kg m^{-3}) that separate the layers in the box inverse model. The corresponding water masses in subtropical and subpolar North Atlantic are labelled to the approximate range of layers.

Layer	Lower surface (γ_n in kg m^3)	Water masses in the subtropics	Water masses in the SPNA
1	26.44	Surface water	
2	26.85		
3	27.162	NACW	North Atlantic Water
4	27.38		
5	27.65		
6	27.82	AAIW/MW	
7	27.89		LSW
8	27.975		
9	28.008	UNADW	
10	28.0276		ISOW
11	28.072		
12	28.0923		
13	28.11	LNADW	
14	28.1295		
15	28.141		DSOW
16	28.154	AABW	
17	Bottom		

Table S6. Mean transport of key circulation components. Mean Transport [Sv] of key circulation components and water masse calculated using the inverse model solution of all repeats at the respective sections. The circulation components include Florida Current (FC) and Deep Western Current (DWBC) at 24.5°N; West Greenland Current (WGC), Labrador Current (LC) at the Labrador section; and East Greenland Current (EGC) and North Atlantic Current (NAC) at the eastern SPNA section. The water masses include Antarctic Intermediate Water (AAIW), upper and lower North Atlantic Deep Water (UNADW and LNADW, respectively), Antarctic Bottom Water (AABW), Labrador Sea Water (LSW), and Overflow Waters (OW). Note that the Ekman transport is prescribed in the inverse model and is not adjusted by the model. "-" sign indicates southward transport.

24.5°N		Labrador section		Eastern SPNA section	
Ekman	4.2	Ekman	-0.3	Ekman	-1.5
FC	31.5±0.5	WGC	31.2±5.5	EGC	-30.1±4.0
DWBC	-25.6±2.0	LC	-38.2±6.4	NAC	16.4±2.1
AAIW	2.2±0.5	LSW	-1.7±1.9	LSW	-8.2±4.0
UNADW	-12.6±3.1	OW	1.4±2.3	OW	-5.7±2.5
LNADW	-6.3±1.5	AMOC	1.6±0.8	AMOC	15.5±1.8
AABW	2.4±0.9				
AMOC	16.3±1.2				